UC Santa Barbara

UC Santa Barbara Previously Published Works

Title

Resolving critical degrees of entanglement in Olympic ring systems

Permalink

https://escholarship.org/uc/item/4427m206

Journal

Journal of Knot Theory and Its Ramifications, 25(14)

ISSN

0218-2165

Authors

Igram, Spencer
Millett, Kenneth C
Panagiotou, Eleni

Publication Date

2016-12-01

DOI

10.1142/s0218216516500814

Peer reviewed

eScholarship.org Powered by the California Digital Library
University of California

Journal of Knot Theory and Its Ramifications
Vol. 25, No. 14 (2016) 1650081 (21 pages)
© World Scientific Publishing Company
DOI: 10.1142/S0218216516500814

World Scientific
www.worldscientific.com

Resolving critical degrees of entanglement in Olympic ring systems

Spencer Igram*, Kenneth C. Millett† and Eleni Panagiotou‡

Department of Mathematics,
University of California,
Santa Barbara, CA 93106, USA
**sigram@live.com*
†*millett@math.ucsb.edu*
‡*panagiotou@math.ucsb.edu*

Received 7 May 2016
Accepted 2 September 2016
Published 6 October 2016

ABSTRACT

Olympic systems are collections of small ring polymers whose aggregate properties are largely characterized by the extent (or absence) of topological linking in contrast with the topological entanglement arising from physical movement constraints associated with excluded volume contacts or arising from chemical bonds. First, discussed by de Gennes, they have been of interest ever since due to their particular properties and their occurrence in natural organisms, for example, as intermediates in the replication of circular DNA in the mitochondria of malignant cells or in the kinetoplast DNA networks of trypanosomes. Here, we study systems that have an intrinsic one, two, or three-dimensional character and consist of large collections of ring polymers modeled using periodic boundary conditions. We identify and discuss the evolution of the dimensional character of the large scale topological linking as a function of density. We identify the critical densities at which infinite linked subsystems, the onset of percolation, arise in the periodic boundary condition systems. These provide insight into the nature of entanglement occurring in such course grained models. This entanglement is measured using Gauss linking number, a measure well adapted to such models. We show that, with increasing density, the topological entanglement of these systems increases in complexity, dimension, and probability.

Keywords: Linking; entanglement; Olympic gel; percolation; periodic boundary condition.

Mathematics Subject Classification 2010: 57M25, 92C05, 92C40

1. Introduction

Olympic systems, see Fig. 1, are collections of small ring polymers modeled in one, two, or three-dimensional systems of large spatial extent. In our study, we characterize such systems having filamentary, laminal, and three-dimensional spatial

†Corresponding author.

Fig. 1. Olympic rings.

structures. In addition to their spatial dimension, these structures have aggregate properties that are characterized by the topological linking that exists between pairs (or larger subcollections) of rings. Although, there are alternative strategies to quantify the extent of entanglement, particularly, in dense systems of polymers, we focus on the Gauss linking number [9], in contrast with the topological entanglement arising from physical movement constraints associated to excluded volume or that arising from chemical bonds. The study of the knotting and, most especially, the linking of polymers was discussed by de Gennes [5] in the context of polymer gels. These Olympic gels have been of interest ever since due to their particular properties and their occurrence in natural organisms, e.g. as intermediates in the replication of circular DNA in the mitochondria of malignant cells, in the kinetoplast DNA networks of trypanosomes [2, 4, 6–8, 12, 13], or in chromosome structural organization or segregation into identifiable territories or domains [3]. These are arenas of substantial contemporary research as they remain quite mysterious despite their fundamental significance and the significant effort dedicated to illuminating structure and function. In this research, we study a course grained model in which the constituent individual unknotted circular chains in our simulation model of polymeric rings empolys the so-called θ-conditions, whereby the individual rings are disjoint but neither attract nor repel each other [5]. As a consequence, excluded volume effects due to an intrinsic thickness of the rings are not taken into account despite the relatively dense character of this system in contrast to the dilute solution associated to θ-conditions. One expects that an excluded volume would affect the detail of the physical scale, but would not change the qualitative behavior that is identified here. We note that Kuhn [11] proposed, for entropic reasons, that the shape of random polymer chains at thermodynamic equilibrium should have the shape of a prolate ellipsoid. This has been numerically confirmed [14, 16] and experimentally. One consequence of this molecular asymmetry is the spatial complexity encountered in the study of linking within Olympic systems consisting of such ring molecules independent of excluded volume considerations.

Here, we study model systems which have an intrinsic one, two, or three-dimensional character and consist of such large collections of ring polymers that

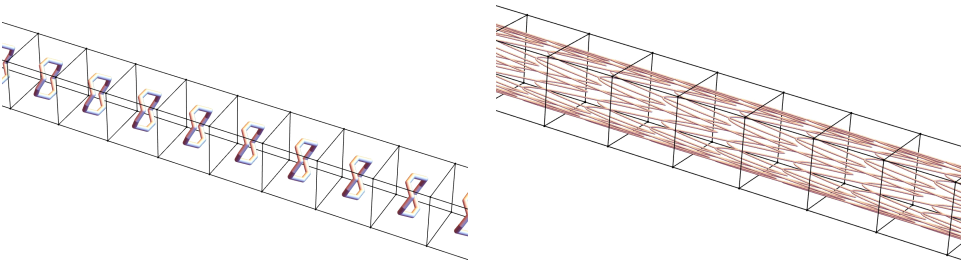

Fig. 2. 1D PBC systems: Unlinked and saturated.

they can be well modeled using systems with periodic boundary conditions. For the one-dimensional, filamentary, case, we impose boundary symmetry on the two faces of the fundamental cell that are perpendicular to the "x" axis, Fig. 2. We characterize the dimensional nature of the large scale topological entanglement and the critical densities at which these first arise by employing periodic boundary condition systems to give a course grained model. The entanglement is measured using the Gauss linking number [9], a measure well adapted to systems employing periodic boundary conditions. In a two-dimensional system, it may occur that there are "parallel" one-dimensional infinite subsystems that are unlinked pairwise but, individually, are linked in a manner that aligns along a single linear subspace, Fig. 3. In other cases, the entire two-dimensional system forms a saturated system, an irreducible linked body, Fig. 3. Similarly, in three dimensions, one may have parallel one-dimensional filamentary linked subsystems, parallel two-dimensional laminal irreducibly linked subsystems, and irreducible infinite three-dimensional linked systems. We show that, with increasing density, the topological entanglement of these systems increases in complexity, dimension, and probability. We identify the critical densities at which these phase changes occur.

In the next section, we will describe periodic boundary condition models and how they are employed in our study of Olympic gels. Next, we describe the linking analysis for periodic boundary condition models via the Gauss linking number. These allow us to identify entangled subsystems, important for the analysis of Olympic systems in the fourth section. In the fifth section, we discuss our summary conclusions.

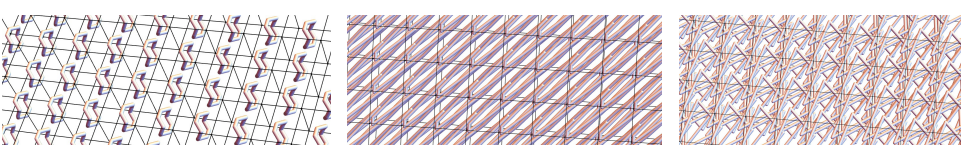

Fig. 3. 2D PBC systems: Unlinked, filamental, and saturated.

2. Olympic Systems via Periodic Boundary Condition (PBC) Models

A one-dimensional system is an array of polymer rings confined to lie in an infinite tube of constant cross-section, see Fig. 2. At low densities, the average character of the one-dimensional PBC system is *totally disconnected* as individual rings are not linked to any others. A one-dimensional system is modeled with one periodic boundary condition by which the basic cell, with symmetric boundary structure, is repeated infinitely, so as to determine an infinite tube with constant cross-section, see Fig. 2. With increasing density, one observes a critical point at which the system becomes a single connected infinite body as there is a chain of linked rings connecting any ring to any other ring. As a function of the density, we determine the average proportion of infinite connected chains.

A two-dimensional system is an array of polymer rings in a two-dimensional PBC system confined to lie between two infinite parallel planes, see Fig. 3. At low densities, one again observes a totally disconnected system of individual rings. As the density increases, one observes the increasing likelihood of a *one-dimensional* infinite connected chain and, with still more density, the presence of a *two-dimensional* infinite connected, or saturated, system of linked rings in which there is a chain of linked rings connecting any ring to any other ring, Fig. 3. By employing two-dimensional PBC systems of closed rings, one has course grained systems that illustrate the complexity that one may encounter. As a function of the density, we quantify and characterize the dimensionality of the linked components of the system.

A three-dimensional system is an array of polymer rings filling a region of, if not the entire, three-dimensional space given by a three-dimensional PBC system, see Fig. 4. Again, at low densities, one observes a totally disconnected system of individual unlinked rings. As the density increases, one first observes the increasing presence of one-dimensional parallel infinite filamental connected systems, then the increasing presence of a two-dimensional parallel laminal infinite connected systems, and then, finally, the presence of a *three-dimensional* infinite connected

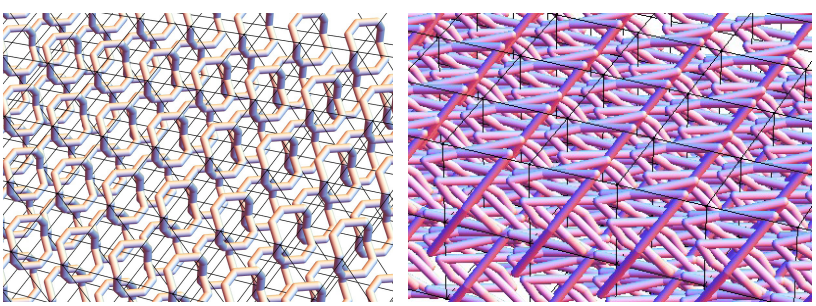

Fig. 4. Unlinked and linked 3D systems: A two layer perspective.

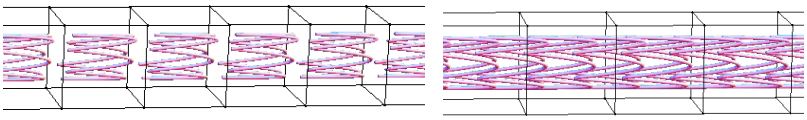

Fig. 5. 1 PBC *low* density and *high* systems achieved with fixed random polygon by changing the cell size.

saturated system. Again, as a function of the density, we quantify and characterize the dimensionality of the linked components of the system.

2.1. *Simulation of Olympic gel systems*

In order to simulate an Olympic gel, we first create an unknotted random 125 edge equilateral polygon using the crankshaft algorithm [1]. The resulting polygon is randomly placed in the interior of a generating cell and extended to a system with 1, 2, or 3 PBC. In order to study the entanglement of the system in different concentrations, we vary the size of the cubic cell in relation to the unchanged polygon by adjusting the distances between the centers of gravity of each image, see Fig. 5. More precisely, we begin with a cubic cell whose edge length is 25 units giving a minimum system density of 0.04 and we vary the density of the system by increments of 0.04 density units. For systems with 1 PBC, oriented along the x-axis, we increase this density scale up to a maximum density of 1.00, therein decreasing both the distances between centers of gravity and the edges parallel to the x-axis from 25 units to 1. For systems with 2 PBC (3 PBC respectively), in the x, y-axes (x, y, z-axes respectively), we achieve a maximum density of 0.72, giving a minimum distance of approximately 1.39 between centers of gravity.

The edge length in each of these systems is proportional to the reciprocal of the varying density, $l = \frac{1}{\rho}$, as the number of vertices in the basic cell will always equal the number of vertices in the polygon but the three-dimensional volume of the cell varies proportionally with the 1, 2, or 3 changing edge lengths, l, for the 1, 2, or 3 periodic boundary condition, respectfully.

3. Linking Entanglement in Olympic Gels Modeled using Periodic Boundary Conditions

In this section, we will discuss the basic ideas that form the theoretical foundation for this study of entanglement in PBC systems as described by Panagiotou [15].

3.1. *PBC systems*

We study a system consisting of a collection of polygonal chains of length n (i.e. of n edges), by dividing the space into a family of rectilinear cuboids of volume abc, where a, b, and c are the side lengths of the cuboid. The structure of the melt in

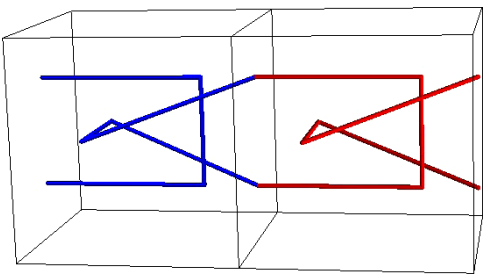

Fig. 6. Two adjacent cells in a 1 PBC model.

each cuboid is identical, i.e. we impose PBC on the system [17]. Specifically, we make the following definition:

Definition 3.1. A *cell* consists of a cuboid with embedded arcs (i.e. parts of curves) whose endpoints lie only in the interior of the cuboid or on the interior of one of its faces, but not on an edge or corner, and those arcs which meet a face satisfy the PBC requirement. That is, to each ending point corresponds a starting point at exactly the same position on the opposite face of the cuboid. See Fig. 6 for an illustrative example of two adjacent cells.

A cell generates a *one, two, or three-dimensional periodic system* in space by tiling the space with the cuboids, so that they fill the space and only intersect on their faces. This allows an arc in one cuboid to be continued across a face into an adjacent cuboid and so on. Notice that the resulting chains may be closed, open or infinite. For a *one-dimensional periodic boundary condition system*, we require that the chain only intersects the interior of the two opposite faces perpendicular to the x-axis. This allows one to fill a one-dimensional solid tube with rectangular cross-section, a filamentous structure. For a *two-dimensional periodic system*, we require that the chain only intersects the interior of the two faces perpendicular to the x-axis or the interior of the two faces perpendicular to the y-axis. This allows one to fill a thickened plane, a laminar structure. Finally, for a *three-dimensional periodic system*, the chain can intersect the interiors of any of the faces but must respect the periodicity constraint. This allows one to fill three space with these cuboids creating a three-dimensional periodic system.

Without loss of generality, we select a cell of the periodic system to be designated as the *generating cell*. A *generating chain* is the union of all the arcs inside the cell, the translations of which define the connected components of the periodic system. For each arc of a generating chain, we choose an orientation such that the translations of all the arcs define a coherently oriented chain in the periodic system. For each generating chain, we choose without loss of generality an arc and a point on it to be its *base point* in the generating cell. An *unfolding* of a generating chain is a connected arc in the periodic system composed by exactly one translation of each

arc of the generating chain. Thus, an unfolding contains exactly one translation and a designated image of a base point of the generating chain. A generating chain is said to be closed (respectively open) when its unfolding is a closed (respectively open) chain. The smallest union of the copies of the cell needed for one unfolding of a generating chain is called the *minimal unfolding*.

The collection of all translations of the same generating chain i is called a *free chain* and is denoted I. A free chain is a union of connected components, each of which is equivalent to any other component under translation. An *image* of a free chain is any arc of a free chain that is the unfolding of a generating chain. The minimal unfolding of I containing an image I_u of I, will be denoted $\mathrm{mu}(I_u)$. For example, in Fig. 6, the blue in the generating cell together with the adjacent red curves determine the closed free chain I that forms $\mathrm{mu}(I_0)$. The image of I whose base point lies in the generating cell is called the *parent image* and denoted I_0. Any other image of I can be defined as a translation of I_0 by a vector $\vec{v}$ from the base point to the base point of the parent image. That is:

$$I_v = I_0 + \vec{v}. \tag{3.1}$$

3.2. *The linking number in PBC systems*

As described, each of the periodic systems consists of an infinite number of chains. So, describing or quantifying the linking number of the chains in the system would appear to require an infinite calculation. Due to the periodicity, however, infinitely many chains have the same conformation, thus their linking is the same. As a consequence, we need only to compute the linking number of all the truly distinct conformations. As we know that the periodic system is generated by one cell, containing only a finite number of generating chains, these can only give rise to a finite number of distinct free chains in the periodic system. We define the linking number at the level of free chains. We notice that an image of a free chain may be entangled with other images of itself, see Fig. 6 for an illustrative example. Thus a measure of entanglement of a free chain must, in general, capture this information as well as the linking with other distinct free chains. In this study, we will generate a single chain and consider its liking with all of its translates arising from the PBC. As a consequence, we give the following, limited, definition of linking for chains in the PBC model employed here. For the general case, we refer to Panagiotou [15]:

Definition 3.2. The Gauss *linking number* of two disjoint (closed or open) oriented curves l_1 and l_2, whose arc-length parametrizations are $\gamma_1(t), \gamma_2(s)$ respectively, is defined as a double integral over l_1 and l_2 [9]:

$$L(l_1, l_2) = \frac{1}{4\pi} \int_{[0,1]} \int_{[0,1]} \frac{(\dot{\gamma}_1(t), \dot{\gamma}_2(s), \gamma_1(t) - \gamma_2(s))}{\|\gamma_1(t) - \gamma_2(s)\|^3} dtds, \tag{3.2}$$

where $(\dot{\gamma}_1(t), \dot{\gamma}_2(s), \gamma_1(t) - \gamma_2(s))$ is the triple product of $\dot{\gamma}_1(t), \dot{\gamma}_2(s)$ and $\gamma_1(t) - \gamma_2(s)$.

In our PBC model, each chain is translated to give an infinite collection copies of itself. As a consequence, we count the number of times a chain, l_0, has a nonzero Gauss linking number with each of the infinitely many translation copies of itself. In an Olympic PBC system, each chain is a compact closed ring and, as a consequence, is contained within finitely many cells. Rings that do not intersect the union of these finitely many cells must have a zero linking number with the ring. Since, only finitely many rings can intersect a cell and there are only finitely many cells containing the chain, there are only finitely many rings that can have a nonzero linking number with it. The *valence* of a ring is the number of rings with which it has a nonzero linking number. Therefore, in our case of Olympic systems, the valence of each chain is finite. While there are situations in which rings can be topologically linked, e.g. the Whitehead link or the Borromean rings, without having a nonzero Gauss linking number these structures have not been observed in our data and are expected to be quite rare in random pairs and triples of random rings. As a consequence, the Gauss linking number is likely a statistically robust detector of linking in Olympic systems.

3.3. *Subsystems and entanglement*

Definition 3.3 (Definitions for one, two, and three dimensions). *Percolation in one dimension* means that the chains organized in one direction are linked to form an infinite connected chain. In such a system, we can imagine the chains form an infinitely long tube containing the connected chains. If such a filamentous tube is contained in a two or three-dimensional system, they form an infinite family of tubes that are disconnected from each other.

Percolation in two dimensions means that the chains along two independent dimensions are linked to form an infinite connected set. In such a system, we can imagine the chains as forming laminar (planar) structures of connected chains. However, these layers are disconnected from each other in a three-dimensional system.

Percolation in three dimensions means that the chains along three independent dimensions are linked to form an entire global infinite connected set.

Definition 3.4 (Percolation cluster, saturated network). An infinite connected component in 1 dimension (1 or 2 dimensions respectively) in a 2 PBC system (3-PBC respectively) respectively, is called a percolation cluster. A 1, 2, or 3 dimensional connected component in a 1, 2, or 3 PBC system respectively is called a saturation network in $1, 2$, or 3 dimensions respectively.

Notice that, in a system generated by one chain in 3 PBC, the existence of a 1-dim (respectively 2-dim) percolation cluster implies the existence of infinitely many 1-dim (respectively 2-dim) percolation clusters and that there are no finite connected components in the system. In a system generated by one chain, the

existence of percolation in 3-dim implies that all the chains are connected to each other, forming a saturation network.

Definition 3.5. Let I_0 denote a chain in a three PBC system generated by a cubic cell and let V be the set of vectors, $\vec{v} \in l\mathbb{Z}^3$ such that $L(I_0, I_0 + \vec{v}) \neq 0$. We define the *valence* of a chain to be the cardinality of V, denoted $|V|$. Thus, the valence of I_0 is the number of images with which the chain has a nonzero linking number.

Remark 3.6. (i) Notice that, due to the periodicity of the system, $|V|$ is independent of the image of I that is used to define it.

(ii) Notice that the valence of a system generated by one chain in 1, 2, or 3 PBC respectively, can be at least 2, 4, or 6 respectively.

(iii) Let M denote the matrix whose columns are the vectors in V, then the system has percolation in k dimensions iff $\text{rank}(M) = k$.

(iv) If one has a cuboid PBC system, instead of a cubic PBC system, one has an analogous set of definitions and results.

4. Analysis of Olympic Systems

In one, two, and three-dimensional Olympic gel systems there is a critical density required for an infinite entangled collection of rings to occur at all. Beyond this critical density, one can determine the probability with which an infinite entangled collection of rings occurs. Such infinite collections can have an intrinsic dimensionality that is lower than that of the entire system. For example, one can have an infinite linear sequence of linked or entangled chain of rings much like that of a necklace. While this is the most complex structure that can arise in a 1 PBC system, we will show that these arise in two and three-dimensional systems creating an infinite fibrous substructure having special structural consequences. In three dimensions, we will show that infinite laminar two-dimensional systems can arise that create a distinctly different structure with distinctly different consequences.

We focus on chains of length $N = 125$. For self avoiding linear rings, the mean square radius of gyration is given by: $\langle R_g^2 \rangle^{1/2} = \sqrt{\frac{N+1}{12}} \approx 3.24$ in chains of this length. It is known that the linear dimensions (span) along the three principle axes of rotation of the cumulative shapes of unknotted polygons using the SBA method, for $N = 125$, $\lambda_1 = 5.97$, $\lambda_2 = 4.09$, $\lambda_3 = 2.90$ [14, 16]. Note that the ellipsoidal reference frame actually has a random orthogonal spatial orientation unaligned with the coordinate axes of the PBC system. The ellipsoidal character of the chains explains, for example, the presence of a filamental structure in an Olympic gel for a range of densities followed by, for another range of densities, of a laminar structure until the dominating three-dimensional saturation of the system. The former are, therefore, likely not aligned with the PBC axes.

4.1. *Analysis of linking*

In this section, we analyze the mean absolute linking of two polygons in a percolated system. In the following, the mean absolute linking number in fact denotes two averages: First, for each configuration, it is the average absolute linking number between a polygon and all its translations and, second, the average over all configurations at the same density.

4.1.1. *Analysis of the mean absolute linking number for* 1 PBC *systems*

The mean absolute linking number in saturated systems in 1 PBC becomes greater than zero at density $\rho \approx 0.08$, when the mean valence and the probability of percolation become nonzero, as expected, see Fig. 7. It is interesting to notice that the mean absolute linking number exceeds one, showing that, even though the polygons are not knotted and are just close enough to link, there exist polygons with absolute linking greater than one. At the critical density, the mean absolute linking becomes 1.3, indicating the presence of many pairs of polygons with absolute linking number greater than one. The mean absolute linking number continues to increase with density, approaching the value 2. This suggests that at high densities unknotted polygons can have high linking numbers. This is supported by the growth of the total absolute linking as a function of the density.

4.1.2. *Analysis of the mean absolute linking number for* 2 PBC *systems*

The mean absolute linking number in saturated systems in 2 PBC becomes greater than zero at density $\rho \approx 0.12$, when the mean valence and the probability of saturation become nonzero, see Fig. 8. It is interesting to notice that the mean absolute linking number exceeds one, showing that, even though the polygons are not knotted and are just close enough to link, there exist polygons with absolute linking greater than one. At the critical density, the mean absolute linking becomes 1.4, indicating the presence of many pairs of polygons with absolute linking number greater

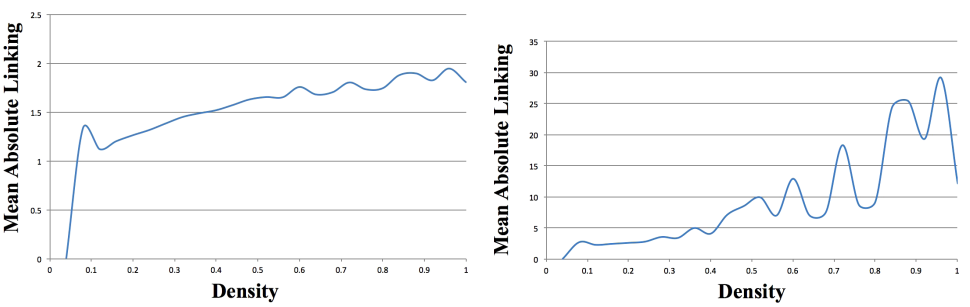

Fig. 7. The mean absolute linking of two chains and the mean total absolute linking per chain as a function of density for 1 PBC saturated systems.

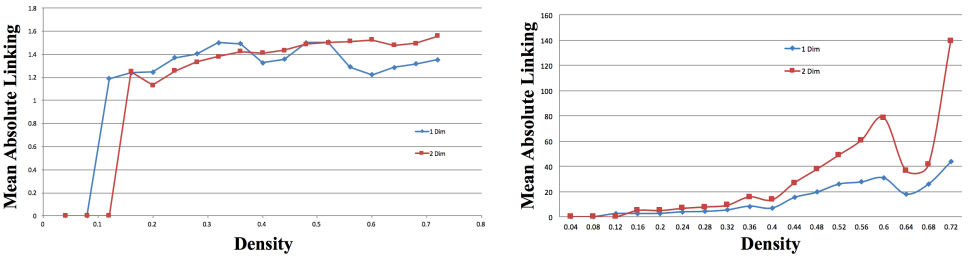

Fig. 8. The mean absolute linking of two chains and the mean total absolute linking per chain as a function of density for 2 PBC saturated systems.

than one. The mean absolute linking number continues to increase with density, approaching the value 2. This suggests that at high densities unknotted polygons can have high linking numbers. This is supported by the growth of the total absolute linking as a function of the density. For $\rho < 0.32$, the mean absolute linking number of one-dimensional percolated systems is greater than the mean absolute linking number of saturated systems, while for $\rho > 0.52$, the opposite holds.

4.1.3. *Analysis of the mean absolute linking number for* 3 PBC *systems*

Figure 9 shows the mean absolute linking number between two components in a percolated system in 1, 2, or 3 dimensions in a system with 3 PBC. The mean absolute linking number of polygons in one-dimensional percolated systems in 3 PBC, becomes nonzero at $\rho \approx 0.12$. As observed in the 1 and 2 PBC systems, it immediately attains values greater than 1, indicating the existence of polygons with linking greater than one. The mean absolute linking number of the saturated systems at the critical saturation density is 1.3. For $\rho \leq 0.24$, the mean absolute linking number is greater for one-dimensional percolated systems than for two-dimensional percolated systems and saturated systems. For $0.24 < \rho < 0.3$, the mean absolute linking number of the one-dimensional percolated systems is greater than that of the saturated systems. For $\rho \leq 0.36$, the mean absolute linking number of the two-dimensional percolated system is greater than that of the saturated systems.

4.2. *Percolation analysis*

For our PBC systems, we propose the following relationship between the probability of total saturation as a function of the density of the system:

$$p(\rho) = \frac{1}{1 + \rho^{-\alpha} e^{-k\rho}}$$

as inspired by the logistic equation, where ρ is the density, $\alpha = n + \frac{1}{2}$, n is the dimension of the PBC system, and k is a constant. A polygon can link with one of its translations when the size of the simulation box is similar to the size of the

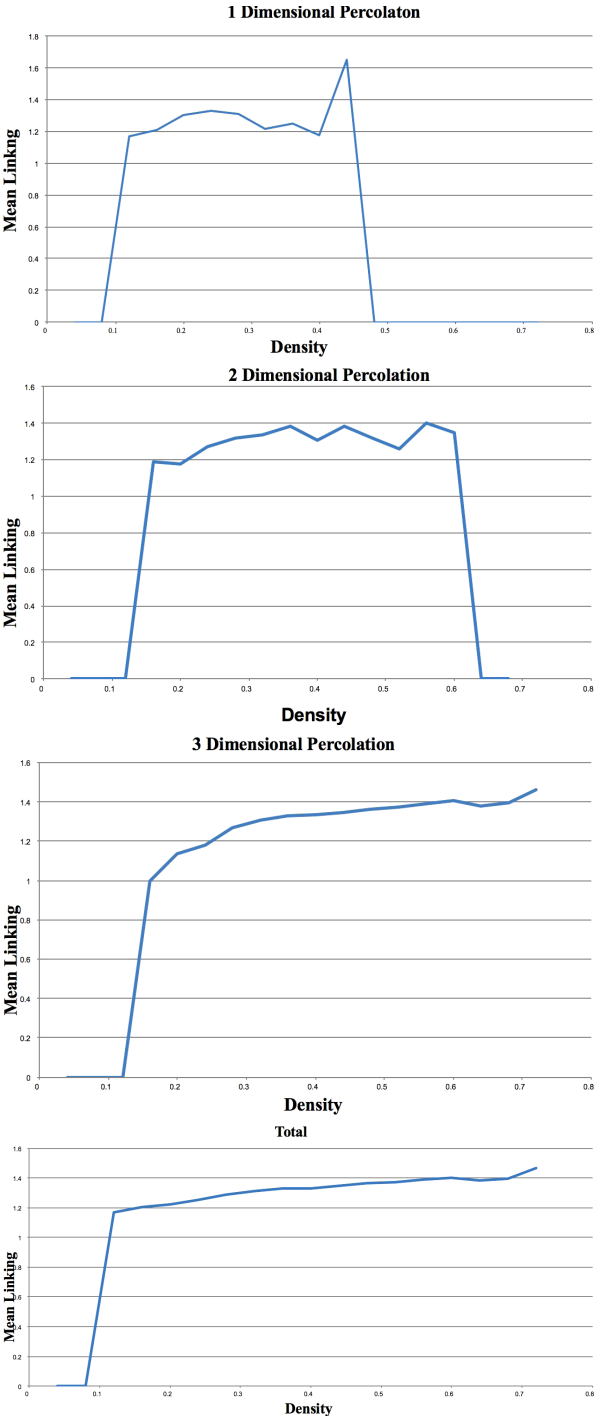

Fig. 9. Mean absolute linking per two chains as a function of density for 3 PBC percolated systems of different dimensions and for all percolated systems.

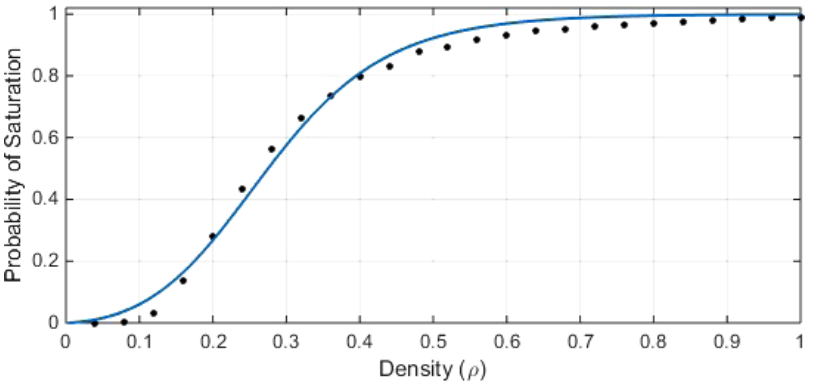

Fig. 10. Probability of saturation in a one-dimensional PBC system as a function of density plotted against its fitting curve $p(\rho)$.

chain. On average, a polygon will link with its own image when the length of the simulation cell is $l \approx 2\langle R_g^2 \rangle^{1/2} \approx 2 \cdot 3.23 = 9.12$, which corresponds to a density of $\rho = \frac{1}{6.45} = 0.15$ for rings. More precisely, in a system with one, two, or three PBC, when the length of the cell is $l < 2\lambda_n$. This implies that, we should expect filamental linking to occur when $l \leq 2\lambda_1$, laminar percolation to occur when $l \leq 2\lambda_2$ and network percolation to occur, where $l \leq 2\lambda_3$. These give critical densities of: $\rho_{C1} > \frac{1}{11.94} = 0.0837521$, $\rho_{C2} > \frac{1}{8.18} = 0.122249$, and $\rho_{C3} > \frac{1}{5.8} = 0.172414$.

4.2.1. *Analysis of one-dimensional systems*

In a one-dimensional PBC system, see Fig. 10, we notice that the probability of saturation becomes greater than 0 at $\rho \approx 0.12$, in agreement with our analysis. In a one-dimensional PBC system, more than half of the conformations are fully saturated once the density has exceeded 0.28. Using *Matlab*'s nonlinear fitting, we find $k = 7.032$ with an $R^2 = 0.9918$, see Fig. 10.

This suggests that the probability of linking between two translations of a polygon as a function of density is:

$$p(\rho) = \frac{1}{1 + \rho^{-1.5} e^{-7.032\rho}}$$

to be compared with the probability of linking between two random unknotted polygons provided in [10].

4.2.2. *Analysis of two-dimensional systems*

In the two-dimensional PBC system, one observes the presence of one-dimensional filamental subsystems and, with increased density, the dominating presence of two-dimensional fully saturated systems. The probability of one-dimensional percolation becomes greater than zero at $\rho \approx 0.12$ and the probability of saturation becomes

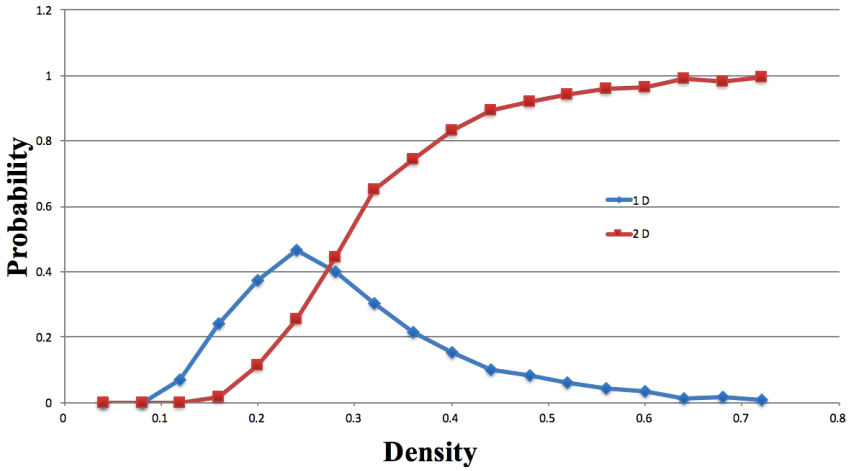

Fig. 11. Probability of one-dimensional and two-dimensional percolation in a two-dimensional PBC system as a function of density.

greater than zero at about $\rho \approx 0.16$, in agreement with our analysis. The probability of one-dimensional percolated subsystems reaches a maximum of $\rho \approx 0.47$, when the density is ≈ 0.26, see Fig. 11. It is interesting to notice that this is the saturation density of 1 PBC systems. At $\rho \approx 0.27$, we notice that the probability of one and two-dimensional percolation (saturation), thus the probability of percolation and saturation, is the same, about 0.4.

In a two-dimensional PBC system, more than half of the conformations are fully saturated once the density has exceeded $\rho \approx 0.28$. Applying *Matlab*'s nonlinear fitting with $\alpha = 2.5$, we find $k = 10.23$ with an $R^2 = 0.9962$, Fig. 12.

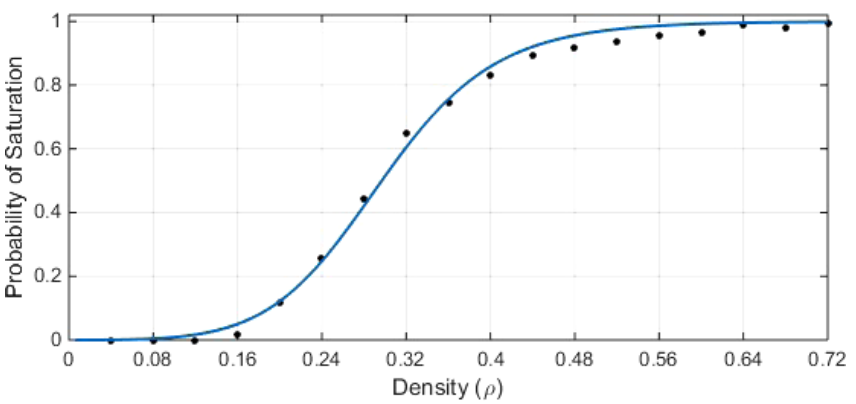

Fig. 12. Probability of saturation in a two-dimensional PBC system as a function of density plotted against its fitting curve $p(\rho)$.

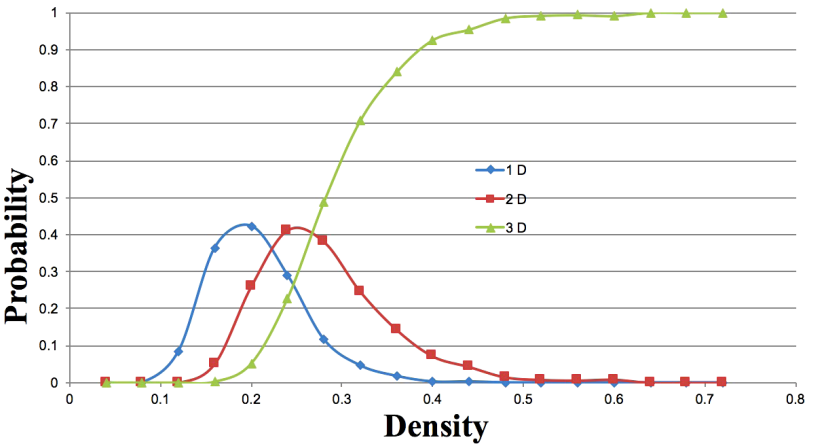

Fig. 13. Probability of one, two and three-dimensional percolation in a three-dimensional PBC system as a function of density.

4.2.3. *Analysis of three-dimensional systems*

In the three-dimensional PBC system, one observes the presence of one, then two-dimensional percolated systems and, later, the three-dimensional fully saturated systems. The probability of filamental and laminar percolation becomes nonzero at $\rho \approx 0.12$ and $\rho \approx 0.16$, respectively, and the probability of saturation (three-dimensional percolation) becomes statistically significant at $\rho \approx 0.20$; all of which are in agreement with the analysis for $\rho_C^{n\,\mathrm{PBC}}$. The probability of both one and two-dimensional percolation reach their maxima of approximately 0.4, when the density is 0.18 and 0.26, respectively. Between these maxima, at $\rho = 0.225$, the probability of one and two-dimensional percolation is the same, equal to 0.35. At density $\rho \approx 0.26$, the probability of two and three-dimensional percolation (i.e. saturation) is the same, equal to 0.4 and, after that, the proportion of three-dimensional saturated systems dominates, see Fig. 13.

In a three-dimensional PBC system, more than half of the conformations are fully saturated once the density has exceeded 0.28. Using *Matlab*'s nonlinear fitting with $\alpha = 3.5$, we find $k = 15.41$ with an $R^2 = 0.9982$, see Fig. 14.

4.2.4. *Comparison of systems across dimensions*

Our numerical results confirm that the percolation probabilities become nonzero when the dimensions of the cell becomes less than twice the average principal axes of the characteristic ellipsoid, respectively, for a polygon of 125 edges. In each dimension, one observes the characteristic saturation density threshold of $\rho \approx 0.28$ at which there is a rapid increase to full saturation. Let us denote the saturation density in 1, 2 and 3 PBC systems as $\rho_s^{1\,\mathrm{PBC}}, \rho_s^{2\,\mathrm{PBC}}, \rho_s^{3\,\mathrm{PBC}}$, respectively. Then $\rho_s^{1\,\mathrm{PBC}} \approx \rho_s^{2\,\mathrm{PBC}} \approx \rho_s^{3\,\mathrm{PBC}} \approx 0.28$. In both 2 and 3 dimensions, one observes

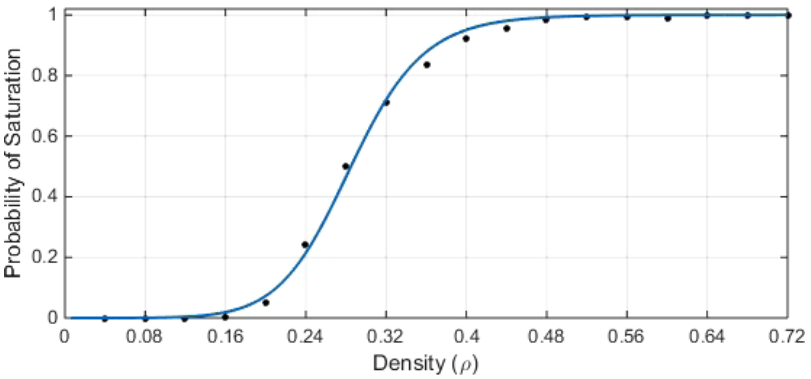

Fig. 14. Probability of saturation in a three-dimensional PBC system as a function of density plotted against its fitting curve $p(\rho)$.

the distinctive initial appearance of lower-dimensional filamental systems whose existence is quickly overwhelmed by the higher-dimensional laminar systems. Let us denote $(\rho_{1d}^{2\,\mathrm{PBC}})_{\max}$, $(\rho_{1d}^{3\,\mathrm{PBC}})_{\max}$, $(\rho_{2d}^{3\,\mathrm{PBC}})_{\max}$ the densities at which the 1-dim (1 and 2-dim, respectively) percolation is maximum in a 2 PBC (respectively, 3 PBC) system. We saw that $(\rho_{1d}^{2\,\mathrm{PBC}})_{\max} \approx (\rho_{2d}^{3\,\mathrm{PBC}})_{\max} \approx \rho_s^{1\,\mathrm{PBC}} \approx 0.26$ and $(\rho_{1d}^{3\,\mathrm{PBC}})_{\max} \approx \frac{1}{\lambda_3} \approx 0.17$. These peaks are less than 0.5 for 2 and 3 PBC systems. At $\rho = 0.27$, the probability of second-order percolation is equal to the probability of saturation in both 2 and 3 PBC.

4.3. *Analysis of valence, $|V|$*

In this section, we discuss the mean valence, $|V|$, of a polygon in a percolated system, i.e. the average number of polygons with which an individual polygon may link. Recalling that the typical enveloping ellipsoid has characteristic radii of $\lambda_1 = 5.97, \lambda_2 = 4.09$, and $\lambda_3 = 2.9$, let us denote by I_0 a random polygon of N unit length edges in a system with n =1, 2, or 3 PBC and defined by its generating cell of dimensions l_x, l_y, l_z. We propose that I_0 may link any of its own translations if the enveloping ellipsoid of the translation intersects the enveloping ellipsoid of I_0. To obtain an estimate of the valence, we first consider the enveloping ellipsoid of I_0 and form a shell around it by adding a thickness proportional to the characteristic radii in the nearest direction i.e. $\lambda_n \frac{\langle Rg^2\rangle^{1/2}}{\lambda_1}$. The respective radii defining this shell are then $(\lambda_1 + \lambda_1 \frac{\langle Rg^2\rangle^{1/2}}{\lambda_1})$, $(\lambda_2 + \lambda_2 \frac{\langle Rg^2\rangle^{1/2}}{\lambda_1})$, $(\lambda_3 + \lambda_3 \frac{\langle Rg^2\rangle^{1/2}}{\lambda_1})$. We estimate the valence by counting the number of images whose center of gravity are contained within this volume by dividing by the volume of the generating cell. Setting the static dimensions of the generating cell equal to $2 * \lambda_n$, we find the following estimates for mean valence in an n-PBC system:

$$\langle |V| \rangle_{n\text{-PBC}} \leq \frac{\frac{4}{3}\pi\lambda_1\lambda_2\lambda_3(1 + \frac{\langle Rg^2\rangle^{1/2}}{\lambda_1})\rho^n}{(2\lambda_{n+1})^{(3-n)}}.$$

Using the appropriate values of n, we bound the mean valence in each system of PBC's by:

$$\langle |V| \rangle_{1\text{PBC}} \leq 16.28\rho$$

$$\langle |V| \rangle_{2\text{PBC}} \leq 296.61\rho^2$$

$$\langle |V| \rangle_{3\text{PBC}} \leq 1089.03\rho^3.$$

We expect these to be upper bound estimates, especially at higher densities, due to the over counting of some portion of cells whose centers are not within the shell. However, the combined volume of those on the boundary of the shell could add to this count.

4.3.1. *Analysis of valence in* 1 PBC *systems*

The mean valence of a saturated system in 1 PBC becomes nonzero at 2 for $\rho \geq 0.12$ corresponding with the critical density for filamental percolation $\rho_{C1} > 0.0836$. The mean valence continues to increase nonmonotonically thereafter, see Fig. 15. Notice that, at the saturation density of $\rho = 0.28$, we have a mean valence of approximately 2.53, indicating that at least a fourth of the linked polygons link with their second-order neighbors. This saturation density corresponds to an edge length of $l \approx 3.57 < 2\lambda_1$, which explains why the mean valence becomes greater than two.

4.3.2. *Analysis of valence in* 2 PBC *systems*

The mean valence of a filamental subsystem in 2 PBC becomes nonzero at $\rho = 0.12$, which corresponds to our analysis of $\rho_C 1 > 0.0836$, where it is steady at 2 through $\rho \approx 0.2$ after which the mean valence begins to increase monotonically (with exceptions at $\rho = 0.4$ and $0.6 \leq \rho \leq 0.68$). The mean valence of the two-dimensional saturated system in 2 PBC becomes nonzero, obtaining a initial value of 4, at $\rho = 0.16$, agreeing with the analysis of $\rho_{C2} > 0.1223$, then increasing monotonically (with similar exceptions as discussed previously for filamental percolation).

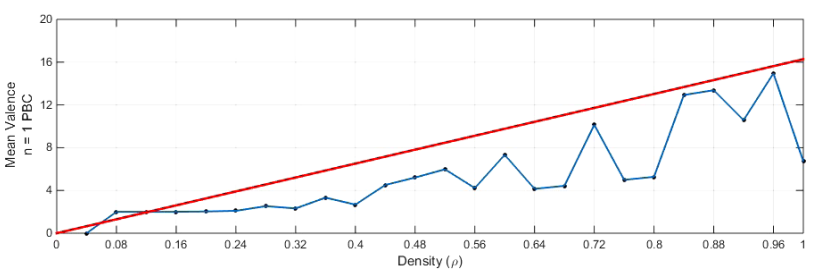

Fig. 15. Mean valence of the total 1 PBC system superimposed with the analytical model. We notice that $\langle |V| \rangle_{1\,\text{PBC}} \leq 16.28\rho$, as expected.

At the saturation density $\rho = 0.28$, the mean valence of the filamental and laminar structures achieve values of approximately 3 and 5.8, respectively. This indicates that, on average, approximately half of the chains in either situation link with their second-order neighbors in some way. Note the difference between the average valence associated to the one-dimensional structure and that of the two-dimensional structure arising from the increased complexity of the entangled network of closed chains, Fig. 16. Another striking feature is the paired decrease in the mean valence of one and two-dimensional systems due to the transformation of one-dimensional systems into two-dimensional systems at a density of $\rho \approx 0.64$ which is where the probability of filamental percolation is less than 0.01.

4.3.3. *Analysis of valence in* 3 PBC *systems*

While the 2 PBC system provides some evidence of the passage to full saturation by passing through an intermediary (one dimensional) subsystem, the passages of

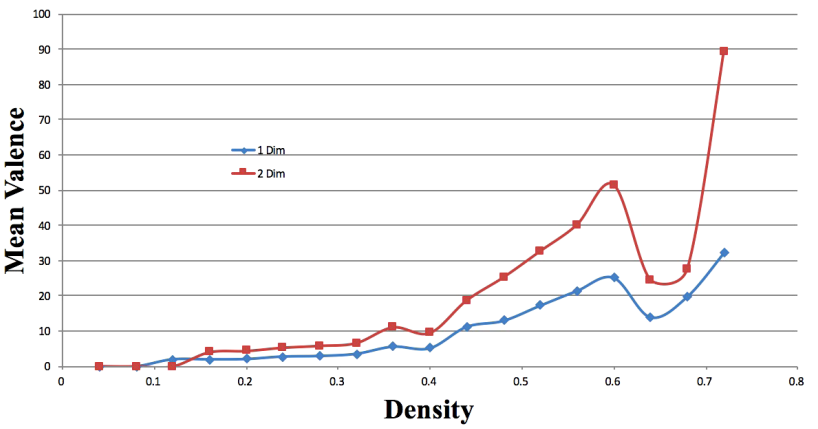

(a)

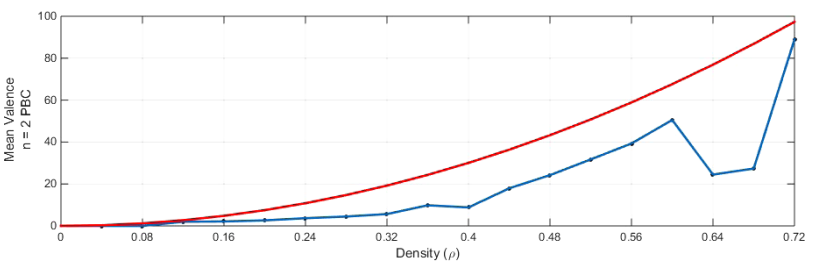

(b)

Fig. 16. (a) Mean valence separated by (1, 2-dimensional) subsystem as a function of density for 2 PBC systems, respectively. (b) Mean valence of the total 2 PBC system bounded by the analytical models. We notice that $\langle V \rangle_{2\,\mathrm{PBC}} \leq 296.61\rho^2$, as expected.

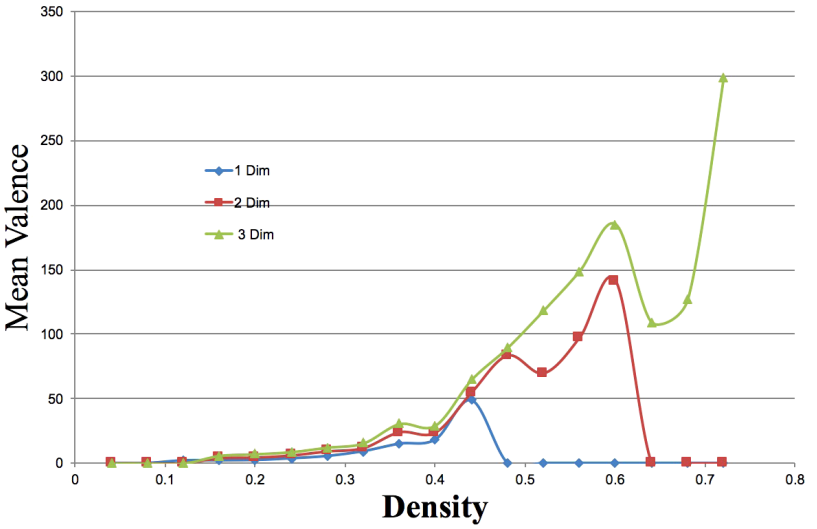

(a)

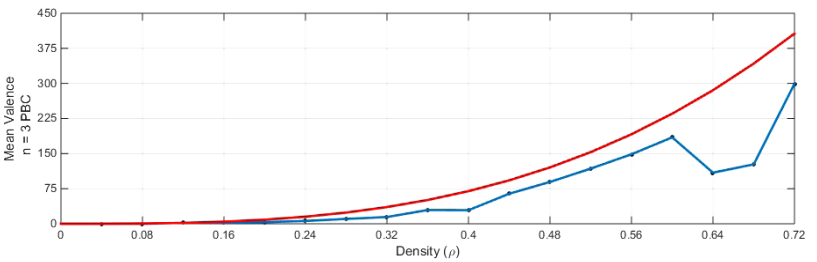

(b)

Fig. 17. (a) Mean valence separated by (1, 2, 3-dimensional) subsystem as a function of density for 3 PBC systems, respectively. (b) Mean valence of the total 3 PBC system superimposed with the analytical model. We notice that $\langle V \rangle_{3\,\mathrm{PBC}} \leq 1089.03\rho^3$, as expected.

the 3 PBC system via one and two-dimensional intermediary subsystems before reaching saturation are even more striking, see Fig. 17. First, we observe the initial filamental percolation beginning at density $\rho = 0.12 > \rho_{C1}$, the laminar percolation beginning at density $\rho = 0.16 > \rho_{C2}$, and the initial occurrence of a statistically weak three-dimensional saturation ($p(\rho) < 0.005$) at $\rho = 0.16$, with a significant probability of saturation beginning at $\rho = 0.20 > \rho_{C3}$. The initial onset of infinite linked structures is briefly stabalized at 2, 4, 8, respectively. At 0.44, the one-dimensional structure becomes all but nonexistent and, at 0.64, the two-dimensional structure vanishes completely. To be more precise, they are transformed into a higher-dimensional structure(s). Note, as in the 2 PBC case, this phase change causes a simultaneous drop in the average valence of the $n+1$ dimensional structure into which it is transformed.

We see significant saturation of the three-dimensional systems beginning at $\rho = 0.2$ and a corresponding monotonic increase in the mean valence for saturated systems (with exceptions at aforementioned transformation points of $\rho \approx 0.4$ and $0.64 < \rho < 0.68$). At the critical saturation density of $\rho = 0.28$, the mean valence for each of the subsystems is greater than 5 and 9, respectively, indicating that more than half the chains in the filamental subsystem are linking with their third order neighbors and over a fourth of those in the laminar subsystems are doing the same. The mean valence of the saturated systems is greater than 12 at this density, suggesting that across all dimensions of percolation, we have at least half of all entangled chains linking with their second-order neighbors or higher. Furthermore, the total system has a mean valence greater than 10 giving even further evidence supporting this statement.

5. Discussion and Conclusions

We have simulated one, two, and three-dimensional systems of deformed circles to provide periodic boundary condition models for macromolecular systems consisting of random unknotted polymer rings. Our study of the linking present in these molecular systems, with varying density, has demonstrated an interesting topological evolution of the infinite saturated subsystems exhibiting dimensional phase transitions as a function of density. We have refined the one, two, and three-dimensional character of these saturated subsystems and identified the fine structure of this transition to saturation with increasing density in one-dimensional filamentous systems, in two-dimensional laminal systems, and in the full three-dimensional systems. We propose that these are a consequence the typical ellipsoidal shape of such ring polymers.

The dimensional phase transitions of the topologically entangled subsystems in our course grained periodic boundary condition model have consequences for biological and physical systems consisting of macromolecular rings such as mitochondria of malignant cells, the kinetoplast DNA networks of trypanosomes, or in chromosome structural organization or segregation into identifiable territories or domains. As the ring macromolecules are unknotted, in these systems, it is fortunate that the linking number is able to capture the entanglement that is present. From an experimental perspective, one might ask if these phase transitions can be observed in such biological systems and, if so, can one alter the density sufficiently to attain beneficial pharmacological consequences? Similarly, are there artifacts of these phase transitions observable in chromosome structure as a consequence of varying density? These are quite fundamental structural questions whose resolution could have important biological consequences. As a consequence, it will be important to consider further research employing mathematical simulations with stronger biophysical and biological features. An interesting first step would be to study a periodic boundary condition model in which each chain is subjected to a random perturbation of controlled magnitude thereby creating a textitquasi-periodic course grained model. Much more challenging but of fundamental importance would be

a model of this character that incorporates excluded volume constraints thereby respecting this critical facet of the macromolecules biophysical properties.

Acknowledgments

Thanks to Javier Arsuaga and Yuanan Diao for helpful discussions.

References

[1] S. Alvarado, J. A. Calvo and K. C. Millett, The generation of random equilateral polygons, *J. Stat. Phys.* **143**(1) (2011) 102–138.
[2] J. Arsuaga, Y. Diao and K. Hinson, The effect of angle restriction on the topological characteristics of minicircle networks, *J. Stat. Phys.* **146**(2) (2012) 434–445.
[3] F. Berger and P. K. Geyer, Editorial overview: Genome architecture and expression: Connecting genome composition and nuclear architecture with function, *Curr. Opin. Genet. Dev.* **37** (2016) iv–vi.
[4] J. Chen, C. A. Rauch, J. H. White, P. T. Englund and N. R. Cozarelli, The topology of kinetoplast dna network, *Cell* **80** (1995) 61–69.
[5] P.-G. De Gennes, *Scaling Concepts in Polymer Physics* (Cornell University Press, 1979).
[6] Y. Diao, K. Hinson and J. Arsuaga, The growth of minicircle networks on regular lattices, *J. Phys. A: Math. Theor.* **45**(3) (2012) 035004.
[7] Y. Diao, K. Hinson, R. Kaplan, M. Vazquez and J. Arsuaga, The effects of density on the topological structure of the mitochondrial dna from trypanosomes, *J. Math. Biol.* **64**(6) (2012) 1087–1108.
[8] Y. Diao, K. Hinson, Y. Sun and J. Arsuaga, The effect of volume exclusion on the formation of dna mini circle networks: implications to kinetoplast dna, *J. Phys. A: Math. Theor.* **48** (2015) 1–11.
[9] K. F. Gauss, Zur mathematischen theorie der electrodynamischen wirkungen, in *Werke*, Vol. 5 (Königliche Societät der Wissenschaften, Gottingen, 1877), p. 605.
[10] N. Hirayama, K. Tsurusaki and T. Deguchi, Linking probabilities of off-lattice self-avoiding polygons and the effects of excluded volume, *J. Phys. A: Math. Theor.* **42** (2009) 105001.
[11] W. Kuhn, Über die gestalt fadenförmiger moleküle in lösungen, *Kolloid Z.* **68** (1934) 2–15.
[12] J. Lukes, D. L. Guilbride, J. Votypka, A. Zikova, R. Benne and P. T. Englund, Kinetoplast dna network: Evolution of an improbable structure, *Eukaryot. Cell* **1**(4) (2002) 495–502.
[13] C. Micheletti, D. Marenduzzo and E. Orlandini, Polymers with spatial or topological constraints: Theoretical and computational results, *Phys. Rep.* **504** (2011) 1–73.
[14] K. C. Millett, P. Plunkett, M. Piatek, E. J. Rawdon and A. Stasiak, Effect of knotting on polymer shapes and their enveloping ellipsoids, *J. Chem. Phys.* **130**(16) (2009) 165104.
[15] E. Panagiotou, The linking number in systems with periodic boundary conditions, *J. Comput. Phys.* (2015).
[16] E. J. Rawdon, J. C. Kern, M. Piatek, P. Plunkett, A. Stasiak and K. C. Millett, Effect of knotting on the shape of polymers, *Macromolecules* **41**(21) (2008) 8281–8287.
[17] M. Rubinstein and R. Colby, *Polymer Physics* (Oxford University Press, 2003).